

Methanol tolerant electrocatalysts for the oxygen reduction reaction

M. Asteazaran · S. Bengiό · W. E. Triaca ·
A. M. Castro Luna

Abstract Direct methanol fuel cells (DMFCs) represent an interesting alternative in obtaining electricity in a clean and efficient way. Portable power sources are one of the most promising applications of passive DMFCs. One of the requirements in these devices is to use high alcohol concentration, which due to methanol crossover causes a considerable loss of fuel cell efficiency. In order to develop methanol tolerant cathodes with suitable activity, different supported catalysts namely PtCo/C and PtCoRu/C, were prepared either via ethylene glycol reduction (EG) with or without microwave heating assistance (MW) or via the alloy method, the latter followed by a thermal treatment in a reducing atmosphere (N_2/H_2). All cathode-catalysts were tested to determine the role of the components in simultaneously enhancing the oxygen reduction reaction (ORR) and discouraging the methanol oxidation reaction. According to the synthesis methodology, X-ray photoelectron spectra showed that the amount of metal oxides on the surface varies, being higher on the PtCo/C EG and PtCoRu/C EG catalysts. The electrochemical characterization of the catalysts was accomplished in a three electrodes electrochemical cell with a glassy carbon rotating

disk electrode covered with a thin catalytic film as working electrode. To study the ORR and the influence of different methanol concentrations, linear sweep voltammetry and cyclic voltammetry were employed. The PtCo/C EG, with an important metal oxide amount on the surface, and the PtCoRu/C MW and EG electrodes, both with RuO_2 on their surfaces, were the most tolerant to methanol presence.

Keywords ORR · PtCo/C · PtCoRu/C · Methanol crossover · DMFC · Methanol-tolerant cathode catalysts

1 Introduction

Direct methanol fuel cells (DMFCs) are an interesting alternative to obtain electricity in a clean and efficient way to substitute traditional environmentally harmful energy sources [1, 2].

One of the most promising applications of DMFCs is as power source in portable devices. In particular, passive alcohol fuel cells using high alcohol concentration have been proposed [3, 4].

Unfortunately, methanol permeation across the polymer electrolyte membrane (methanol crossover) causes a considerable loss of efficiency in the cell, because both the oxygen reduction reaction (ORR) and the methanol oxidation reaction (MOR) occur simultaneously at the cathode.

Numerous attempts have been proposed to find a solution to the problem by either synthesizing novel ion conducting membranes resistant to alcohols [5, 6] or by making electrocatalysts with high activity for the ORR and at the same time tolerant to alcohol presence [7–9]. Platinum is considered as the most active catalyst for ORR in acid media, however due to kinetic limitations of the

M. Asteazaran · W. E. Triaca · A. M. Castro Luna
Instituto de Investigaciones Físicoquímicas Teóricas y Aplicadas (INIFTA), Facultad de Ciencias Exactas, UNLP-CONICET, La Plata, Argentina

S. Bengiό
Centro Atómico Bariloche, Comisión Nacional de Energía Atómica (CAB-CNEA) and CONICET, Bariloche, Argentina

A. M. Castro Luna (✉)
Centro de Investigación y Desarrollo en Ciencia y Tecnología de Materiales (CITEMA), Facultad Regional La Plata, UTN, La Plata, Argentina
e-mail: castrolu@inifta.unlp.edu.ar; castrolu@gmail.com

reaction, mostly due to Pt-oxide formation, materials with high catalytic activity are required for low temperatures fuel cells to compensate the low efficiency of the kinetic process [10, 11].

It has been claimed that by alloying platinum with certain transition metals M (M = Co, Fe, Cr, Ni) it is possible to improve the Pt activity for the ORR due to the cocatalysts causing a downward shift of the Pt d-band center with respect to the Fermi level, thus diminishing the adsorption strength of the oxygen species. The improvement for the ORR has been demonstrated with PtM alloys prepared by different procedures [11–13].

Moreover, in DMFCs, problems related to catalytic activity of the cathode are more severe since methanol competes with oxygen for the active Pt sites and a mixed potential emerges from the simultaneous occurrence of the ORR and MOR reactions. Different Pt base nanoparticles have been proposed and employed for ORR in presence of methanol [14–16]. In Ref. [17], Ocón et al. claimed that a methanol tolerant catalyst, namely PtCoRu/C, can be obtained in an operating DMFC after Ru dissolution of a PtRu anode and its subsequent deposition on the PtCo/C cathode.

The use of different procedures to synthesize metal nanoparticles supported on carbon of high surface area plays an important role in the development of fuel cell technology. Special attention should be paid not only on the catalyst composition but also on the synthesis method employed in their preparation [12, 18].

The aim of this work is to synthesize by different routes carbon supported nanoparticles of PtCo/C and PtCoRu/C as methanol tolerant oxygen reduction catalysts and to discern the causes of improvements in their methanol tolerance.

2 Materials and methods

2.1 Preparation and characterization of the catalysts

Carbon supported nanoparticles (NP) of PtCo/C and PtCoRu/C were prepared by using either (i) the classic ethylene glycol method (EG) [19] and a variation with microwave-assisted heating (MW) or (ii) the alloy method (AM), in line with Gonzalez et al. [20].

2.1.1 Classic EG and microwave heating assisted MW methods

In the classic EG, ethylene glycol is the reducing agent and dissolving medium where the synthesis occurs. Summarizing, ethylene glycol solutions of each metal precursor, H_2PtCl_6 , CoCl_2 and RuCl_3 , in the required amount were

added in a suspension of a calculated amount of functionalized carbon black support in ethylene glycol, under vigorous stirring. The mixture was stirred for 4 h under N_2 bubbling. Once the stirring was finalized, NaOH solution in ethylene glycol was added to the mixture to adjust its pH around 13. In order to achieve complete reduction of the metallic precursors, the mixture was refluxed at 197 °C for 2 h also under N_2 bubbling. The solid was isolated by low pressure filtering, then thoroughly rinsed with water and dried at 70 °C in an oven for 12 h. The synthesized electrocatalysts were labeled as PtCo/C EG and PtCoRu/C EG. Additionally, functionalization of the support was achieved after oxidative treatment in 70 % HNO_3 solution at 140 °C for 2 h, according to the work of Bonesi et al. [21].

In the ethylene glycol microwave-assisted heating procedure (MW), PtCoRu/C MW was prepared following the method described by Almeida et al. [22]. Following this method, a calculated amount of the different precursors was added in ethylene glycol and stirred for approximately 5 min in an ultrasonic bath, and a measured amount of carbon Vulcan[®] XC-72R powder was then added. The mixture was kept under ultrasound stirring for 30 min, until a homogeneous suspension was obtained. This suspension was then placed in a common household microwave oven (Likon, 2.45 GHz, 700 W) and irradiated for 70 s. Finally, the suspension was filtered and washed repeatedly with water, and then dried in an oven at 80 °C for 12 h.

2.1.2 Alloy method

In the AM, the initial reactant was a given quantity of E-TEK Pt/Vulcan XC-72R, which was dispersed in water and ultrasonically stirred for 15 min. The initially acidic pH was shifted to 8 by adding an ammonium hydroxide solution. At this point, the required amount of CoCl_2 , in order to obtain the compositions listed in Table 1, was put into the mixture and then, a HCl solution was added to reach a pH of 5.5. Stirring continued for 1 h and then the solid was isolated by filtering, rinsing with water repeatedly and finally drying at 70 °C in an oven for 12 h. After that, the powder was heat-treated at 900 °C in a H_2/N_2 atmosphere for 1 h to form a binary alloy catalyst. The synthesized electrocatalysts were labeled as PtCo/C AM.

2.2 Catalysts characterization

2.2.1 Physicochemical characterization

All synthesized materials were studied in terms of composition and surface chemistry by using energy-

Table 1 Summary of the properties of the investigated catalysts

Synthesis method	Pt/Co at. ratio ^a	Pt/Ru at. ratio ^a	Catalyst label	SA ^b [mA cm ⁻²]	MA ^c [Amg _{Pt} ⁻¹]	ECSA ^d [m ² g _{Pt} ⁻¹]	Onset ORR ^e [V]
EG	5.2		Pt ₅ Co EG	0.18	0.07	40.06	0.837
AM	5.3		Pt ₅ Co AM	0.24	0.19	79.79	0.867
EG	10.1		Pt ₁₀ Co EG	0.12	0.06	49.86	0.842
AM	10.4		Pt ₁₀ Co AM	0.33	0.30	90.66	0.875
EG	3.1	1.1	PtCoRu EG	0.11	0.05	44.68	0.829
MW	8.3	1.2	PtCoRu MW	0.19	0.11	58.92	0.859

^a Determined from EDS analysis

^b Specific activity for ORR in an O₂ saturated 0.5 M H₂SO₄ calculated at 0.8 V

^c Mass activity for ORR in an O₂ saturated 0.5 M H₂SO₄ calculated at 0.8 V

^d Electrochemically active surface area

^e Onset potential for ORR determined from Fig. 2

dispersive X-ray spectroscopy (EDS) and X-ray photoelectron spectroscopy (XPS).

For the surface composition analysis via XPS a standard Al/Mg twin anode X-ray gun and a hemispherical electrostatic electron energy analyzer were used. For the analysis, the powdered samples were spread on an adhesive carbon tape and the C 1 s peak at 284.5 eV was used as reference to calibrate the binding-energy scale.

2.2.2 Electrochemical characterization

The electrochemical characterization was accomplished by employing a standard three-electrode electrochemical cell. We used as a working electrode a rotating disk electrode (RDE) of glassy carbon (0.071 cm² geometric area) covered with a thin layer of catalyst powder (28 μg cm⁻² Pt loading), attached by a Nafion[®] thin film [23]. A Pt foil of 1 cm² geometric area was used as counter electrode and a saturated calomel electrode (SCE) as reference electrode. In this work, we refer all potentials to that of the reversible hydrogen electrode (RHE). The supporting electrolyte used was 0.5 M H₂SO₄ and the working solution was an O₂ saturated 0.5 M H₂SO₄ solution containing different CH₃OH concentrations. The electrochemical experiments were conducted at room temperature. Prior to all experiments, we cycled the potential of the working electrode between 0.05 and 1.10 or 0.8 V (depending on the catalyst composition) at a rate of 0.1 Vs⁻¹ in a N₂ purged 0.5 M H₂SO₄ solution in order to get a stable voltammetric profile.

The electrochemically active surface area of each working electrode, listed in Table 1, was then determined by integrating the charge required for stripping a pre-adsorbed monolayer of CO at 0.05 V, taking into account that 420 μC is equivalent to 1 cm².

3 Results and discussion

3.1 Physicochemical characterization

3.1.1 EDS analysis

The atomic percentages of the components in PtCo/C and PtCoRu/C EG, MW and AM catalysts, listed in Table 1, were determined by EDS. It can be highlighted that EDS is a surface technique that goes through <1 μm whereas XPS measures the elemental composition of the surface from the top to 4 nm in depth.

3.1.2 XPS analysis

The surface composition of the catalysts was determined measuring the Pt 4f, Co 2p and Ru 3d photoelectron peaks. The XPS spectra of Pt based catalysts Pt₅Co/C AM, Pt₅Co/C EG, PtCoRu/C MW and PtCoRu/C EG obtained in the region of Pt 4f core level, are shown in Fig. 1a, b, c and d, respectively. Each of these elemental spectra is composed of two identical peaks that correspond to the spin-orbit split 4f 7/2 and 4f 5/2 of Pt. We identified up to three components in each spectrum which are ascribed to elemental Pt(0) and Pt-oxides species, presumably PtO and PtO₂.

For the Pt₅Co/C AM in Fig. 1a, we identified a single component at binding energies, BE = 71.2 eV, ascribed to Pt(0). As expected the AM catalysts submitted to an H₂/N₂ atmosphere at high temperature allow getting metallic Pt [20]. For the Pt₅Co/C EG catalyst in Fig. 1b, we identified two additional components to Pt(0), at 72.3 and 74.3 eV ascribed to PtO and PtO₂ [24]. For the PtCoRu/C MW catalyst in Fig. 1c and for the PtCoRu/C EG catalyst in Fig. 1d, we also identified two additional components to Pt(0), at BE = 73.3 eV and at BE = 75.4 eV. Here it is

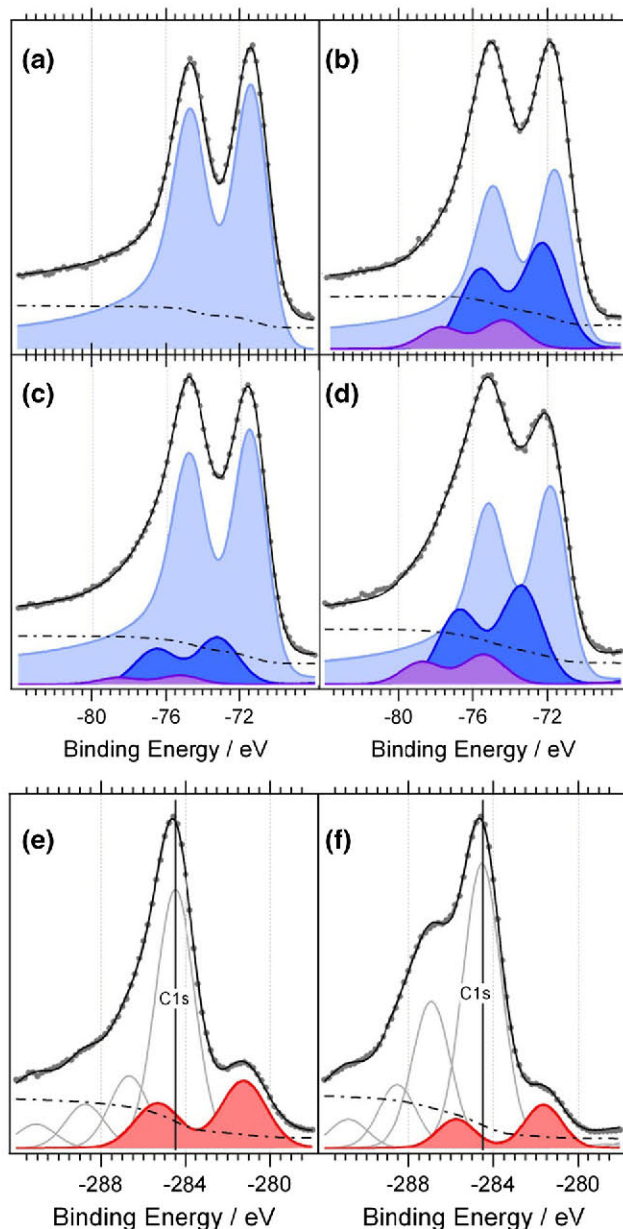


Fig. 1 XPS spectra of Pt 4f from **a** Pt₅Co/C AM **b** Pt₅Co/C EG **c** PtCoRu/C MW **d** PtCoRu/C EG and of Ru 3d from **e** PtCoRu/C MW and **f** PtCoRu/C EG

Table 2 XPS determined percentage (% wt) of metallic Pt and Pt-oxides

Catalyst	Metallic Pt [% wt]	Pt-oxides [% wt]
Pt ₅ Co/C AM	100	0
Pt ₁₀ Co/C AM	100	0
PtCoRu/C MW	86	14
PtCoRu/C EG	65	35
Pt ₁₀ Co/C EG	66	34
Pt ₅ Co/C EG	62	38

worth noting that extra components are shifted apart 1 eV to more bounded states in both PtCoRu/C with respect to the nominal values of PtO and PtO₂. This shift has been already reported in the literature [25, 26]. Jung et al. [27] analyzing Pt-oxide thin films in the region of Pt 4f core level have also reported a component at 73.3 eV ascribed to the formation of an intermediate oxide, probably Pt₂O₃-like.

The contribution to the Pt 4f raw spectra of the peaks corresponding to the Pt-oxides is 14 % in the PtCoRu/C synthesized by MW method and in those catalysts obtained by the EG method reached almost 40 % as shown in Table 2.

In regard to Ru, the XPS spectra of PtCoRu/C catalysts were analyzed in the region of the Ru 3d core-level peak, which partially overlaps with the C 1 s core-level peak. Each of these elemental spectra is composed of two identical peaks for Ru, which correspond to the spin-orbit split 3d 5/2 and 3d 3/2 (with relative intensities 3:2), and for C a single peak 1 s, for each component. For PtCoRu/C MW and PtCoRu/C EG the XPS spectra of Ru are shown in Fig. 1e and f respectively. We identified a single component of Ru 3d at BE = 281 eV for the PtCoRu/C MW catalyst, and at BE = 281.5 eV for the PtCoRu/C EG catalyst (the existence of only a single component was also corroborated by measuring the Ru 3p peak, not shown). The Ru 3d peaks for the PtCoRu/C MW catalyst can be assigned to RuO₂ (280.8 eV), and although in the PtCoRu/C EG catalyst it is shifted from the bulk binding energy of RuO₂, it could still be assigned to it due to final state effects because of the small size of NP [28]. This final state effect produces binding energy shifts to more bound states. This core level shifts of small metallic NP over poor conducting substrates comes from the positive charge that remains in the NP once created the electron-hole pair during the photoemission process, as this charge is not neutralized in times relevant to photoemission due to the weak NP-substrate interaction.

Besides the single Ru 3d component, in Fig. 1e and f, several C 1 s components are plotted. The XPS peak deconvolution of C 1 s shows four single peaks, at ca. 284.5 eV, 287 eV, 288.5 eV and 291 eV, which could be assigned according to increasing binding energy values: C=C (284.45 eV) and C-C (285.3 eV) for the signal at 284.5 eV; C-O (286.9 eV) and >C=O (287.2 eV) for the signal at 287 eV; -COO (288.96 eV) for the peak at 288.5 eV; and ester group (292.3 eV) for the peak at 291 eV [29, 30].

The Co 2p XPS spectra (not shown) of the synthesized catalysts exhibit peaks with binding energies that can be assigned to Co (0) (778.3 eV), Co(OH)₂ (781 eV), and CO₃O₄ or CoO at (780.3 eV) [24].

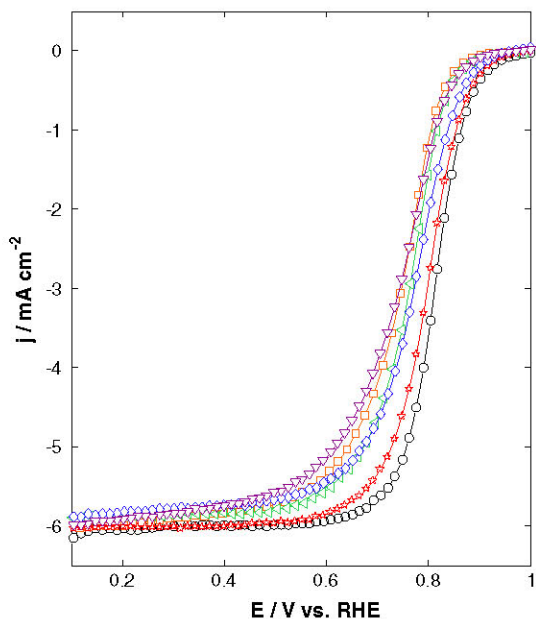


Fig. 2 Polarization curves for ORR in O_2 saturated 0.5 M H_2SO_4 at $v = 0.005 \text{ Vs}^{-1}$ and $\omega = 2,000 \text{ rpm}$ on $Pt_{10}Co/C$ AM (○), Pt_5Co/C AM (★), $PtCoRu/C$ MW (◇), Pt_5Co/C EG (▶), $Pt_{10}Co/C$ EG (◀) and $PtCoRu/C$ EG (◻) catalysts. (Color figure online)

In all cases the spectra were fitted using a Voigt function for each peak plus a Shirley-type background. The total fitted intensities along with the experimental ones are shown in each spectrum.

3.2 Electrochemical characterization

To assess the activity for ORR we recorded polarizations curves at different rotation rates between 1.0 and 0.2 V scanning the working electrode potential at a rate of 0.005 Vs^{-1} (LSV). The current densities of the polarization curves shown in this work were calculated taking into account the geometric area of the electrode. The background current was measured by running the polarization curves under identical conditions as the LSV for ORR, under N_2 -purged 0.5 M H_2SO_4 solution. This background current was subtracted from the experimental ORR current to eliminate any contributions of capacitive current. Typical polarizations curves for ORR on $Pt_{10}Co/C$ AM and EG, Pt_5Co/C AM and EG, $PtCoRu/C$ EG and $PtCoRu/C$ MW electrodes at a rotating disc rate $\omega = 2,000 \text{ rpm}$ are shown in Fig. 2a, b and c, respectively. In order to determine the electrocatalytic activity of each electrode, the current values of the polarization curves for the ORR were used to calculate according to Koutecky-Levich the kinetic current at $E = 0.8 \text{ V}$. The specific activity (SA) and mass activity (MA) values of the tested electrode are listed in Table 1. It is noticed, that EG catalysts exhibit lower MA and ECSA

values than those of AM and MW catalysts. The reason of this behavior can be the smaller amount of metallic Pt in EG catalysts. Further investigation would be necessary to fully understand these results. The onset potential, at which the current for oxygen reduction is first observed, was determined by the point of intersection of two lines, one drawn extending the baseline (i.e. from 1 to 0.9 V) and the other extending the increasing linear portion of ORR curve, the onset potential for each catalysts is shown in Table 1. The superposition of the ORR polarization curves confirmed that the catalysts exposed to a reducing atmosphere, AM catalysts, alongside with MW catalyst have the highest onset potential for the ORR, due to the same reason written right above, i.e. the smaller amount of metallic Pt in EG catalysts.

To find out how the composition and the synthesis method of the electrode materials influence the methanol tolerance, we measured the polarization curves in O_2 saturated 0.5 M $H_2SO_4 + 0.1 \text{ M } CH_3OH$ at $\omega = 2,000 \text{ rpm}$ with the different catalysts. We show in Fig. 3a the polarization curves for the ORR employing $Pt_{10}Co/C$ EG and AM and in Fig. 3b those on Pt_5Co/C EG and AM. It is clear from the figures that the AM catalysts show less methanol tolerance [31] and that the amount of Co has also an influence on methanol tolerance, i.e. higher Co amount diminishes the MOR [32]. From the electrocatalytic behavior of the tested electrodes, we conclude that the best catalyst for ORR is not the most tolerant to methanol presence. Polarization curves for the ORR on $PtCoRu/C$ EG and $PtCoRu/C$ MW, which are shown in Fig. 3c, exhibit a remarkable high methanol tolerance. It seems that the presence of Ru in the catalyst has contributed to increase the alcohol tolerance, XPS results identify a unique species RuO_2 , which has been found to be less active for methanol oxidation [33, 34].

It is important to point out that the requirements demanded for a suitable cathode catalyst are: (i) good catalytic behavior for the ORR and (ii) high tolerance to methanol presence. Therefore, not only the synthesis method but the composition of the catalysts are important in order to obtain a suitable cathode catalyst. In Fig. 4a, for $Pt_{10}Co/C$ EG, and in Fig. 4b, for $PtCoRu/C$ EG the polarization curves for ORR in the presence of different amount of methanol are shown. Notice that $Pt_{10}Co/C$ EG, despite being obtained by the same method that $PtCoRu/C$ EG, shows that higher concentrations of methanol makes it less resistant. To confirm these results, the following investigation on the electrocatalytic behavior of $PtCoRu/C$ and $PtCo/C$ catalysts for methanol oxidation, in a N_2 saturated 0.1 M $CH_3OH + 0.5 \text{ M } H_2SO_4$ solution, was carried out by cyclic voltammetry. In Fig. 5 are shown the current density-potential profiles on $Pt_{10}Co/C$ AM and $PtCoRu/C$ EG, the current densities are given on the basis

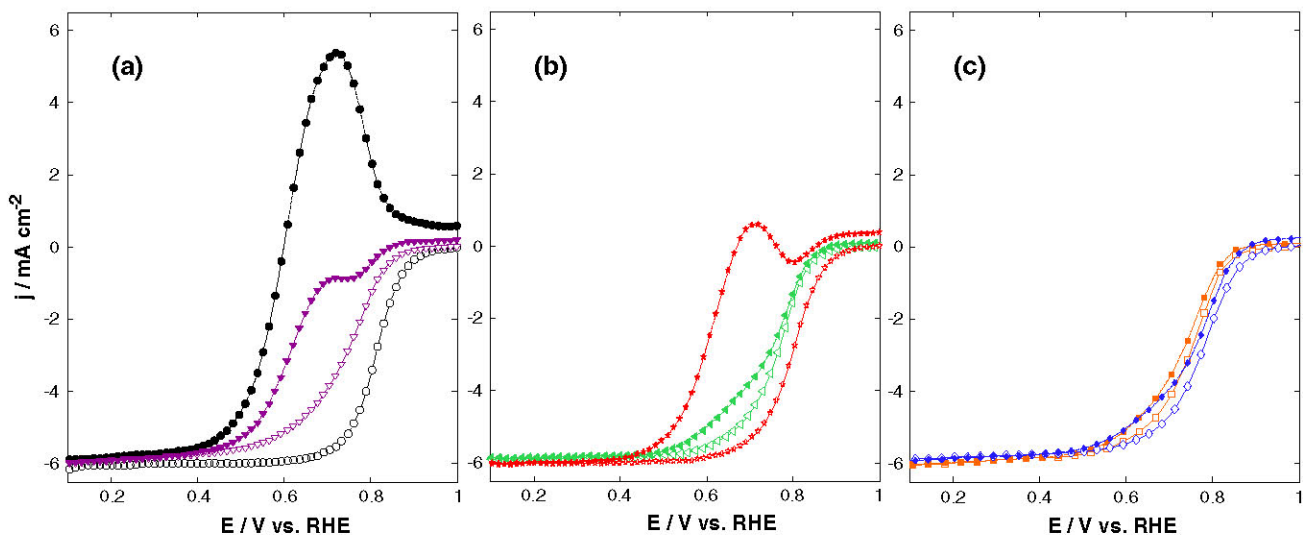
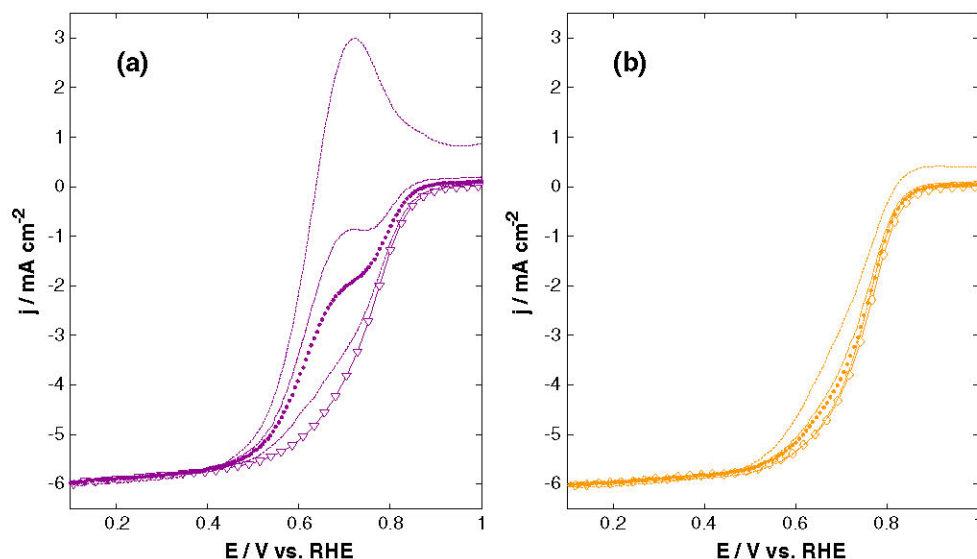


Fig. 3 Polarization curves for ORR in O_2 saturated 0.5 M H_2SO_4 at $v = 0.005 \text{ Vs}^{-1}$ and $\omega = 2,000 \text{ rpm}$ without and with 0.1 M CH_3OH a on $Pt_{10}Co/C$ AM without CH_3OH (\circ) or with 0.1 M CH_3OH (\bullet) and on $Pt_{10}Co/C$ EG without CH_3OH (∇) or with 0.1 M CH_3OH (\blacktriangledown), b on Pt_5Co/C EG without CH_3OH (\triangleright) with 0.1 M CH_3OH (\blacktriangleright) and on Pt_5Co/C AM without CH_3OH (\star) or with 0.1 M CH_3OH (\blackstar) and c $PtCoRu/C$ EG without CH_3OH (\square) or with 0.1 M CH_3OH (\blacksquare) and on $PtCoRu/C$ MW without CH_3OH (\diamond) or with 0.1 M CH_3OH (\blacklozenge). (Color figure online)

Fig. 4 Polarization curves for ORR in O_2 saturated 0.5 M H_2SO_4 with different CH_3OH concentrations at $v = 0.005 \text{ Vs}^{-1}$ and $\omega = 2,000 \text{ rpm}$ a on $Pt_{10}Co/C$ EG without CH_3OH (∇), with 0.01 M CH_3OH (\bullet), with 0.05 M CH_3OH (\circ), with 0.1 M CH_3OH (\blacktriangle), with 0.5 M CH_3OH (\blacktriangledown) and b on $PtCoRu/C$ EG without CH_3OH (\square), with 0.01 M CH_3OH (\blacklozenge), with 0.05 M CH_3OH (\circ), with 0.1 M CH_3OH (\blacktriangle), with 0.5 M CH_3OH (\blacktriangledown). (Color figure online)



of the electrochemically active area. It can be seen that in the increasing potential scan (forward scan), the onset potential for methanol oxidation on $PtCoRu/C$ EG has almost the same value as the one on $Pt_{10}Co/C$ AM (onset potential ca. 0.36 V). In the decreasing potential scan (backward scan) the methanol oxidation peak emerges immediately after the surface oxide reduction happens. In particular, for the $PtCoRu/C$ EG catalyst, the methanol oxidation peak in the reverse scan is located at lower potential value, i.e. 0.50 V, in comparison to 0.65 V for $Pt_{10}Co/C$, indicating a lower electrocatalytic reactivity of

the $PtCoRu/C$ EG catalyst for this alcohol oxidation. From this analysis we conclude that $PtCoRu/C$ EG is not a suitable catalyst for methanol oxidation.

Taking into account the curves shown in Fig. 3, we define the term relative methanol tolerance percentage (RMT %) of the prepared catalysts, considering the ratio of the difference between the current density for ORR with and without methanol at 0.7 V for any catalyst and the same difference on the catalysts with the highest activity for MOR (i.e. $Pt_{10}Co/C$), the calculated ratio for each catalyst is then subtracted from 1 and multiplied by 100.

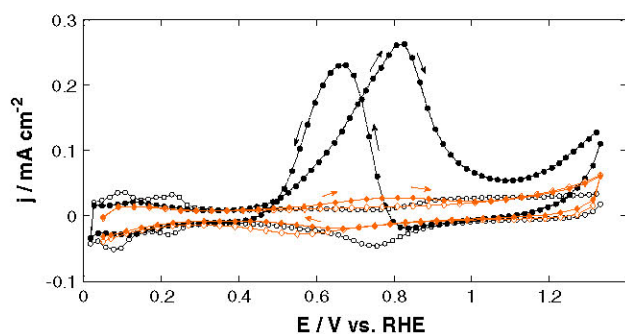


Fig. 5 Cyclic voltammograms for MOR in N_2 purged 0.5 M H_2SO_4 at $v = 0.010 \text{ Vs}^{-1}$ and $\omega = 2,000 \text{ rpm}$ on $Pt_{10}Co/C$ AM without CH_3OH (○) or with 0.5 M CH_3OH (●) and on $PtCoRu/C$ EG without CH_3OH (□) or with 0.5 M CH_3OH (■). (Color figure online)

Table 3 Relative methanol tolerance percentage (RMT %) of the prepared catalysts

Catalyst	RMT % ^a
$Pt_{10}Co/CAM$	0
Pt_5Co/CAM	54.68
$Pt_{10}Co/CEG$	71.78
Pt_5Co/CEG	92.14
$PtCoRu/C$ EG	94.88
$PtCoRu/C$ MW	95.98

^a At 0.7 V in O_2 saturated 0.5 M $H_2SO_4 + 0.1 \text{ M } CH_3OH$

The RMT % of all catalysts are listed in Table 3. Notice that the highest RMT % values correspond to $PtCoRu/C$ catalysts and the lowest value to $PtCo/C$ AM catalysts.

4 Conclusions

- The AM and MW methods allow to get the best catalysts for ORR.
- The AM method used to obtain suitable catalysts for ORR worsens methanol resistance, in contrast to the EG method.
- A higher Co amount in the catalyst composition diminishes methanol oxidation.
- A strong effect on the methanol tolerance is achieved by the addition of Ru in the catalyst composition.

Acknowledgments This work was supported by Consejo Nacional de Investigaciones Científicas y Técnicas (CONICET), Agencia Nacional de Promoción Científica y Tecnológica, Comisión de Investigaciones Científicas de la Provincia de Buenos Aires (CIC), and Universidad Tecnológica Nacional (UTN-FRLP). AMCL is member of the research career at CIC. MA acknowledges financial support from CONICET through a Ph.D. fellowship. The authors acknowledge Dr. A Medina for helpful discussions.

References

1. Aricò AS, Baglio V, Antonucci V (2009) Direct methanol fuel cells: history, status and perspectives. In: Liu H, Zhang J (eds) *Electrocatalysis of direct methanol fuel cells: from fundamentals to applications*. Wiley-VCH Verlag GmbH & Co. KGaA, Weinheim, pp. 1–78. doi:10.1002/9783527627707.ch1
2. Corti HR, Gonzalez ER (2014) *Direct alcohol fuel cells materials performance, durability and applications*. Springer, Amsterdam. doi:10.1007/978-94-007-7708-8
3. Baglio V, Stassi A, Matera FV, Antonucci V, Aricò AS (2009) Investigation of passive DMFC mini-stacks at ambient temperature. *Electrochim Acta* 54:2004–2009. doi:10.1016/j.electacta.2008.07.061
4. Falcão DS, Oliveira VB, Rangel CM, Pinto AMFR (2014) Review on micro-direct methanol fuel cells. *Renew Sustain Energy Rev* 34:58–70. doi:10.1016/j.rser.2014.03.004
5. Antonucci PL, Aricò AS, Cretí P, Ramunni E, Antonucci V (1999) Investigation of a direct methanol fuel cell based on a composite Nafion-silica electrolyte for high temperature operation. *Solid State Ion* 125:431–437. doi:10.1016/S0167-2738(99)00206-4
6. Kim YS, Zelenay P (2009) Polymer electrolyte fuel cell durability. In: Büchi FN, Inaba M, Schmidt TJ (eds) *Direct methanol fuel cell durability*. Springer, New York, pp 223–240. doi:10.1007/978-0-387-85536-3_10
7. Shukla AK, Raman RK (2003) Methanol-resistant oxygen reduction reaction catalysts for direct methanol fuel cells. *Annu Rev Mater Res* 33:155–168. doi:10.1146/amurev.matsci.33.072302.093511
8. Oh J-G, Kim H (2008) Synthesis and characterization of PtN_x/C as methanol-tolerant oxygen reduction electrocatalysts for a direct methanol fuel cell. *J Power Sources* 181:74–78. doi:10.1016/j.jpowsour.2008.02.095
9. Papageorgopoulos DC, Liu F, Conrad O (2007) A study of Rh_xSy/C and Ru_xSe_y/C as methanol-tolerant oxygen reduction catalysts for mixed-reactant fuel cell applications. *Electrochim Acta* 53:1037–1041. doi:10.1016/j.electacta.2007.09.037
10. Zhang J (2008) *PEM fuel cell electrocatalysts and catalyst layers: fundamentals and applications*. Springer, New York. doi:10.1007/978-1-84882-846-9
11. Toda T, Igarashi H, Uchida H, Watanabe M (1999) Enhancement of the electroreduction of oxygen on Pt Alloys with Fe, Ni, and Co. *J Electrochem Soc* 146:3750–3756
12. Spanos I, Kirkensgaard JJK, Mortensen K, Arenz M (2014) Investigating the activity enhancement on Pt_xCo_{1-x} alloys induced by a combined strain and ligand effect. *J Power Sources* 245:908–914. doi:10.1016/j.jpowsour.2013.07.023
13. Murthi VS, Urian RC, Mukerjee S (2004) Oxygen reduction kinetics in low and medium temperature acid environment: correlation of water activation and surface properties in supported Pt and Pt alloy electrocatalysts. *J Phys Chem B* 108:11011–11023. doi:10.1021/jp048985k
14. Antolini E, Lopes T, Gonzalez ER (2008) An overview of platinum-based catalysts as methanol-resistant oxygen reduction materials for direct methanol fuel cells. *J Alloy Compd* 461:253–262. doi:10.1016/j.jallcom.2007.06.077
15. Yang H, Coutanceau C, Léger JM, Alonso-Vante N (2005) Methanol tolerant oxygen reduction on carbon-supported Pt–Ni alloy nanoparticles. *J Electroanal Chem* 576:305–313. doi:10.1016/j.jelechem.2004.10.026
16. Castro Luna AM, Bonesi A, Triaca WE, Baglio V, Antonucci V, Aricò AS (2008) Pt–Fe cathode catalysts to improve the oxygen reduction reaction and methanol tolerance in direct methanol fuel

- cells. *J Solid State Electrochem* 12:643–649. doi:[10.1007/s10008-007-0334-0](https://doi.org/10.1007/s10008-007-0334-0)
17. Escudero-Cid R, Hernández-Fernández P, Pérez-Flores JC, Rojas S, García-Rodríguez S, Fatás E, Ocón P (2012) Analysis of performance losses of direct methanol fuel cell with methanol tolerant PtCoRu/C cathode electrode. *Int J Hydrog Energy* 37:7119–7130. doi:[10.1016/j.ijhydene.2011.12.158](https://doi.org/10.1016/j.ijhydene.2011.12.158)
 18. Lázaro MJ, Celorrio V, Calvillo L, Pastor E, Moliner R (2011) Influence of the synthesis method on the properties of Pt catalysts supported on carbon nanocoils for ethanol oxidation. *J Power Sources* 196:4236–4241. doi:[10.1016/j.jpowsour.2010.10.055](https://doi.org/10.1016/j.jpowsour.2010.10.055)
 19. Grolleau C, Coutanceau C, Pierre F, Leger J (2010) Optimization of a surfactant free polyol method for the synthesis of platinum—cobalt electrocatalysts using Taguchi design of experiments. *J Power Sources* 195:1569–1576
 20. Salgado JRC, Antolini E, Gonzalez ER (2004) Structure and activity of carbon-supported Pt–Co electrocatalysts for oxygen reduction. *J Phys Chem B* 108:17767–17774. doi:[10.1021/jp0486649](https://doi.org/10.1021/jp0486649)
 21. Bonesi AR, Moreno MS, Triaca WE, Castro Luna AM (2010) Modified catalytic materials for ethanol oxidation. *Int J Hydrog Energy* 35:5999–6004. doi:[10.1016/j.ijhydene.2009.12.093](https://doi.org/10.1016/j.ijhydene.2009.12.093)
 22. Almeida TS, Palma LM, Leonello PH, Morais C, Kokoh KB, De Andrade AR (2012) An optimization study of PtSn/C catalysts applied to direct ethanol fuel cell: effect of the preparation method on the electrocatalytic activity of the catalysts. *J Power Sources* 215:53–62. doi:[10.1016/j.jpowsour.2012.04.061](https://doi.org/10.1016/j.jpowsour.2012.04.061)
 23. Paulus UA, Schmidt TJ, Gasteiger HA, Behm RJ (2001) Oxygen reduction on a high-surface area Pt/Vulcan carbon catalyst: a thin-film rotating ring-disk electrode study. *J Electroanal Chem* 495:134–145. doi:[10.1016/S0022-0728\(00\)00407-1](https://doi.org/10.1016/S0022-0728(00)00407-1)
 24. Moulder JF, Stickle WF, Sobol PE, Bomben KD (1992) Handbook of X-Ray photoelectron spectroscopy. Perkin-Elmer Corporation, Waltham
 25. Aricò AS, Shukla A, Kim H, Park S, Min M, Antonucci V (2001) An XPS study on oxidation states of Pt and its alloys with Co and Cr and its relevance to electroreduction of oxygen. *Appl Surf Sci* 172:33–40. doi:[10.1016/S0169-4332\(00\)00831-X](https://doi.org/10.1016/S0169-4332(00)00831-X)
 26. Raman RK, Shukla AK, Gayen A, Hegde MS, Priolkar KR, Sarode PR, Emura S (2006) Tailoring a Pt–Ru catalyst for enhanced methanol electro-oxidation. *J Power Sources* 157:45–55. doi:[10.1016/j.jpowsour.2005.06.031](https://doi.org/10.1016/j.jpowsour.2005.06.031)
 27. Jung MC, Kim HD, Han M, Jo W, Kim DC (1999) X-ray photoelectron spectroscopy study of Pt-oxide thin films deposited by reactive sputtering using O₂/Ar Gas mixtures. *Jpn J Appl Phys* 38:4872–4875. doi:[10.1143/JJAP.38.4872](https://doi.org/10.1143/JJAP.38.4872)
 28. Larichev YV, Moroz BL, Bukhtiyarov VI (2011) Electronic state of ruthenium deposited onto oxide supports: an XPS study taking into account the final state effects. *Appl Surf Sci* 258:1541–1550. doi:[10.1016/j.apsusc.2011.09.127](https://doi.org/10.1016/j.apsusc.2011.09.127)
 29. Okpalugo TIT, Papakonstantinou P, Murphy H, McLaughlin J, Brown NMD (2005) High resolution XPS characterization of chemical functionalised MWCNTs and SWCNTs. *Carbon* 43:153–161. doi:[10.1016/j.carbon.2004.08.033](https://doi.org/10.1016/j.carbon.2004.08.033)
 30. Smirnova AL, Hu YL, Zhang L, Aindow M, Menard P, Singh P, Goberman D, Shaw L, Wan X, Rhine W (2009) Synthesis of novel electrode materials using supercritical fluids. *ECS Trans* 19:9–21. doi:[10.1149/1.3242512](https://doi.org/10.1149/1.3242512)
 31. Taguchi M, Takahashi H, Nakajima S (2013) Methanol oxidation activity and chemical state of platinum oxide thin film treated by electrochemical reduction. *Mater Trans* 54:582–587. doi:[10.2320/matertrans.MBW201215](https://doi.org/10.2320/matertrans.MBW201215)
 32. Salgado JRC, Antolini E, Gonzalez ER (2005) Carbon supported Pt–Co alloys as methanol-resistant oxygen-reduction electrocatalysts for direct methanol fuel cells. *Appl Catal B* 57:283–290. doi:[10.1016/j.apcatb.2004.11.009](https://doi.org/10.1016/j.apcatb.2004.11.009)
 33. Long JW, Stroud RM, Swider-Lyons KE, Rolison DR (2000) How to make electrocatalysts more active for direct methanol oxidation-avoid PtRu bimetallic alloys! *J Phys Chem B* 104:9772–9776. doi:[10.1021/jp001954e](https://doi.org/10.1021/jp001954e)
 34. Ma L, Liu C, Liao J, Lu T, Xing W, Zhang J (2009) High activity PtRu/C catalysts synthesized by a modified impregnation method for methanol electro-oxidation. *Electrochim Acta* 54:7274–7279. doi:[10.1016/j.electacta.2009.07.045](https://doi.org/10.1016/j.electacta.2009.07.045)